

BIOMIMETIC SCAFFOLDS FROM CHEMICALLY
MODIFIED CELLULOSE FOR SKIN TISSUE
ENGINEERING

FARAH HANANI BINTI ZULKIFLI

Thesis submitted in fulfillment of the requirements
for the award of the degree of
Doctor of Philosophy (Advanced Materials)

Faculty of Industrial Sciences & Technology
UNIVERSITI MALAYSIA PAHANG

SEPTEMBER 2015

ABSTRACT

Research using biomaterials as scaffolds in skin tissue engineering is tremendously increasing as these biomaterials have been found to mimic the structure of extracellular matrix (ECM) that provides a platform for cell attachment, differentiation and proliferation. Hydroxyethyl cellulose (HEC) is modified cellulose, one of the most abundant natural polymers in the world. The advantage of HEC is its chemical structure, which exactly matches that of glycosaminoglycan (GAG) in the dermis. The focus of this research is to develop scaffolds based on HEC for skin tissue engineering. Two techniques were used to fabricate scaffolds, which are electrospinning and freeze-drying. Electrospinning produces fibers in nanometer scale and interconnected pores that closely resemble the topography features of ECM. Freeze-drying is an easy and convenient technique to produce highly interconnected pores, favourable in tissue engineering. This report comprised of two parts. The first part is about the fabrication and characterization of scaffolds using electrospinning and freeze-drying techniques while the second part is the cell culture studies of nanofibers and freeze-dried scaffolds. In the first part, there are four different studies conducted based on HEC polymers. The first study is on the effect of cross-linking effect on HEC/PVA and HEC/PVA/collagen nanofiber scaffolds prepared by electrospinning method. The concentration of HEC (5%) with PVA (15%) was optimized, blended in different ratios (30-50%) of HEC content and electrospun to obtain smooth nanofibers. The fabrication of HEC/PVA/collagen (0.38%) was also reported. Nanofibers were made water insoluble through chemical cross-links using glutaraldehyde. The microstructure, morphology, mechanical and thermal properties of the HEC/PVA and HEC/PVA/collagen nanofibrous scaffolds was characterized *via* SEM, ATR-FTIR, DSC, UTM and TGA. The second is the *in vitro* degradation study aimed to investigate the behaviour of electrospun HEC/PVA and HEC/PVA/collagen nanofibrous scaffolds in two biologically related media: phosphate buffered solution (PBS) and Dulbecco's modified Eagle's medium (DMEM) for a 12-week incubation period. The results showed that HEC/PVA/collagen scaffolds degraded slower in both media than HEC/PVA scaffolds. All fibers displayed uneven and rough surfaces towards the final week of incubation periods. As degradation time increased, the thermal studies revealed that the melting temperatures and crystallinity of the scaffolds slightly shifted to a lower value. Both HEC/PVA and HEC/PVA/collagen fibers showed a significant decrease in Young's modulus and tensile stress over the 12-week degradation. The third study is fabrication of biopolymeric scaffolds of HEC and PVA using freeze-dry technique and characterized based on their potential for skin tissue engineering. The pore size of HEC/PVA blended scaffolds (2 - 40 μm) showed diameters in the range of both pure HEC (2 - 20 μm) and PVA (14 - 70 μm) scaffolds. All porous scaffolds revealed porosity above 85 %. The water uptake and degradation rate of HEC scaffolds could be controlled by incorporation of PVA in the blends. The ATR-FTIR results exhibit possible interactions between hydroxyl groups of HEC and PVA in the blends. TGA/DrTGA curves clarified different major steps of weight loss involved with different scaffolds. The T_g values of HEC/PVA of the DSC curve occur in the range of

HEC and PVA, which represents the miscibility of HEC/PVA blend polymers. Higher Young's modulus was obtained by increasing the HEC content. The forth study is the fabrication of novel HEC/silver nanoparticles (AgNPs) formed *via* the freeze-drying using mixture of HEC and AgNO₃ where HEC acts as the reducing agent to silver nanoparticles. Scaffolds from HEC/AgNPs composites were successfully prepared with average pore size ranging from 50 to 150 μ m. The surface Plasmon resonance, which shows absorption peaks in the range of 417 – 421 nm, validates the presence of silver nanoparticles in the HEC matrices. The HEC/AgNPs scaffolds showed significance porosity of more than 80 % and a high degree of swelling ratio properties. The DSC thermogram showed augmentation in T_g with the increase of Ag content. The second major part of this work showed cytotoxicity studies based on investigation of morphology and cell proliferation of scaffolds using SEM and MTT/MTS assays. Cell-scaffolds interaction demonstrated that melanoma and human fibroblast (hFB) cells differentiated and spread well on scaffolds with better cell proliferation and attachment with time, appeared more prominent on HEC/PVA/collagen nanofibers, HEC/PVA freeze-dried and HE/AgNPs (1.6%) scaffolds. Since these biocompatible and biodegradable scaffolds showed promising results, these scaffolds could be adopted for the design of next-generation tissue-engineered skin grafts or wound dressing.

ABSTRAK

Penyelidikan menggunakan biobahan sebagai perancah pada kejuruteraan tisu kulit menunjukkan peningkatan yang ketara memandangkan kesamaan biobahan ini dalam struktur ekstrasellular matriks (ECM) serta menyediakan platform untuk perlekatan, percambahan dan perkembangan sel. Hidroksietil selulosa (HEC) adalah selulosa yang diubahsuai, dan merupakan salah satu polimer semulajadi terbanyak di dunia. Kelebihan HEC terletak pada struktur kimianya yang sepadan dengan glikosaminoglikan (GAGs) pada dermis. Fokus kajian ini adalah untuk membangunkan perancah berasaskan HEC untuk kejuruteraan tisu kulit. Terdapat dua teknik digunakan untuk mengfabrikasi perancah ini iaitu elektroputaran dan beku-pengeringan. Elektroputaran adalah teknik bagi menghasilkan gentian pada saiz nanometer dan menunjukkan ciri-ciri topografi poros saling berhubung yang hampir sama dengan ECM. Selain itu, terdapat juga teknik beku-pengeringan, iaitu teknik yang mudah dan sesuai dalam menghasilkan poros saling berhubung yang tinggi, dimana sangat diperlukan dalam bidang kejuruteraan tisu. Terdapat dua bahagian utama dalam kajian ini. Pertama adalah fabrikasi dan pencirian perancah menggunakan teknik elektroputaran dan beku-pengeringan, dan bahagian kedua adalah kajian kultur sel ke atas perancah gentian nano dan beku-pengeringan dalam aplikasi kejuruteraan tisu kulit. Dalam bahagian pertama, terdapat 4 kajian yang berlainan dijalankan berasaskan polimer HEC. Pertama ialah kajian pautan silang ke atas perancah gentian nano HEC/PVA dan HEC/PVA/ kolagen yang disediakan melalui kaedah elektroputaran. Kepekatan HEC (5%) dengan PVA (15%) telah dioptimumkan, dicampur dalam nisbah yang berbeza (30 - 50%) dan dielektroputar untuk mendapatkan gentian nano yang rata. Fabrikasi pada gentian nano HEC/PVA/kolagen (0.38%) juga turut dilaporkan. Gentian nano dijadikan tidak larut air melalui pautan silang secara kimia menggunakan glutaraldehid. Mikrostruktur, morfologi, sifat mekanikal dan haba perancah gentian nano dari campuran HEC/PVA dan HEC/PVA/kolagen telah dicirikan melalui SEM, ATR-FTIR, DSC, UTM dan TGA. Kajian kedua ialah degradasi secara *in vitro*, yang dilakukan untuk menyelidik ciri-ciri perancah gentian nano HEC/PVA dan HEC/PVA/kolagen dalam dua media biologi: larutan tampan fosfat (PBS) dan media DMEM selama 12 minggu tempoh inkubasi. Keputusan menunjukkan bahawa perancah HEC/PVA/kolagen mempamerkan kadar degradasi yang perlahan dalam kedua-dua media berbanding gabungan gentian nano HEC/PVA. Semua gentian menunjukkan permukaan yang tidak rata dan kasar pada minggu-minggu terakhir tempoh inkubasi. Apabila masa inkubasi meningkat, terdapat beberapa perubahan kecil dalam struktur kimia dimana dipaparkan pada spektrum FTIR manakala kajian terma mempamerkan puncak suhu lebur dan penghabluran perancah sedikit beralih kepada nilai yang lebih rendah. Kedua-dua gentian HEC/PVA dan HEC/PVA/kolagen menunjukkan penurunan yang ketara dalam modulus Young dan tegasan tegangan dalam tempoh 12 minggu degradasi. Kajian ketiga ialah perancah biopolimer daripada HEC dan PVA telah disintesis menggunakan teknik beku-pengeringan dan dicirikan berdasarkan potensi mereka dalam kejuruteraan tisu kulit. Saiz liang daripada perancah gabungan HEC/PVA (2-40 μm) menunjukkan diameter dalam lingkungan perancah HEC (2-20 μm) dan PVA

(14-70 μm) tulen. Semua perancah poros menunjukkan nilai porositi lebih daripada 85%. Penyerapan air dan kadar degradasi perancah HEC boleh dikawal dengan penambahan PVA dalam sebatian matriks polimer. Keputusan FTIR pula menunjukkan interaksi-interaksi kimia yang wujud di antara kumpulan hidroksil HEC dan sebatian perancah komposit. Lengkung TGA/DrTGA memaparkan perbezaan tangga penurunan berat bagi setiap perancah yang berkadar dengan suhu. Nilai T_g bagi lengkung DSC pada HEC/PVA berada diantara HEC dan PVA tulen menunjukkan keterlarutcampuran daripada HEC/PVA polimer campuran. Nilai modulus Young yang lebih tinggi telah diperolehi dengan peningkatan nilai HEC. Kajian keempat, novel nanopartikel HEC/perak (AgNPs) yang terdiri daripada pelbagai kepekatan AgNO_3 dibentuk melalui teknik beku-pengeringan. Larutan HEC digunakan sebagai agen penurunan dalam sintesis nanopartikel perak. Perancah dari HEC dengan nanopartikel perak telah berjaya dihasilkan dengan purata saiz liang antara 50-150 μm . Permukaan Plasmon resonans menunjukkan puncak penyerapan dalam lingkungan 417-421 nm, mengesahkan kehadiran nanopartikel perak dalam matriks HEC. HEC/AgNPs perancah menunjukkan keliangan lebih daripada 80% dan mepamerkan sifat nisbah penyerapan yang tinggi. Thermogram DSC menunjukkan peningkatan di T_g bertambah dengan kepekatan AgNO_3 . Dalam bahagian kedua tesis ini, kajian sitotoksiti telah dilakukan, dimana morfologi dan sel pembiakan perancah diuji menggunakan SEM dan MTT/MTS antibiofilem. Interaksi sel-perancah menunjukkan bahawa sel-sel melanoma dan fibroblas manusia (hFB) membiak dan bercambahan dengan baik berkadar dengan masa, dimana keputusan lebih jelas diperhatikan pada perancah gentian nano HEC/PVA/kolagen, HEC:PVA (1:2) beku-pengeringan dan HEC/AgNPs (1.6%). Oleh kerana perancah bioserasi dan biodegradasi menunjukkan hasil yang memberangsangkan, perancah ini boleh diguna pakai untuk reka bentuk tisu-kejuruteraan generasi akan datang cantuman kulit atau berpakaian luka.

TABLE OF CONTENTS

	Page
SUPERVISOR'S DECLARATION	II
STUDENT'S DECLARATION	III
DEDICATION	IV
ACKNOWLEDGEMENTS	V
ABSTRACT	VI
ABSTRAK	VIII
TABLE OF CONTENTS	X
LIST OF TABLES	XIV
LIST OF FIGURES	XV
LIST OF SYMBOLS	XX
LIST OF ABBREVIATIONS	XXI
CHAPTER 1 INTRODUCTION	1
1.1 Background	1
1.2 Problem statement	3
1.3 Significance of studies	4
1.4 Research objectives	5
1.5 Research scope	5
1.6 Thesis outline	6
CHAPTER 2 LITERATURE REVIEW	7
2.1 Human skin physiology	7
2.1.1 General function of skin	8
2.1.2 Structural and mechanical properties of skin	9
2.2 Skin tissue engineering	10
2.3 Biomaterials in tissue engineering	18
2.3.1 Evolution of biomaterials	18
2.3.2 Characteristics of biomaterials scaffold	20

2.3.3	Biodegradable scaffolds	21
2.3.4	Classification of biomaterials	22
2.3.5	Hydroxyethyl cellulose	25
2.3.6	Poly (vinyl) alcohol	26
2.3.7	Collagen	28
2.4	Overview of nanoparticle	30
2.4.1	Silver nanoparticles	30
2.5	Summary	32
CHAPTER 3	MATERIALS AND METHODS	34
3.1	Research methodology	34
3.2	Materials preparation	35
3.3	Preparation of electrospinning aqueous polymeric solutions	36
3.3.1	Synthesis of HEC/PVA and HEC/PVA/collagen nanofibers scaffolds	36
3.4	Preparation of freeze-dried aqueous polymeric solutions	37
3.4.1	Synthesis of HEC/PVA freeze-dried scaffolds	37
3.4.2	Synthesis of HEC/silver nanoparticles freeze-dried scaffolds	37
3.5	Fabrication techniques	38
3.5.1	Electrospinning	38
3.5.2	Freeze-drying	41
3.6	Characterization technique	43
3.6.1	Scanning electron microscope	43
3.6.2	Attenuated total reflectance-Fourier Transform Infrared Spectroscopy	45
3.6.3	Thermogravimetric analysis	47
3.6.4	Differential scanning calorimetry	49
3.6.5	Mechanical properties	51
3.6.6	Ultraviolet-visible spectroscopy	53
3.6.7	Porosity study	55
3.6.8	Swelling ratio study	55
3.6.9	pH value measurements	56
3.6.10	Swelling ratio study	56
3.6.11	Weight loss study	56
3.7	Cell culture studies	57
3.7.1	Cell expansion and seeding	58
3.7.2	Cell morphology studies	59
3.7.3	A375 melanoma cell proliferation study	59
3.7.4	hFB cell proliferation study.	60
3.8	Statistical analysis	61

CHAPTER 4	FABRICATION AND CHARACTERIZATION OF SCAFFOLDS USING ELECTROSPINNING AND FREEZE-DRYING TECHNIQUES	62
4.1	CHEMICALLY CROSSLINKED STUDY OF HEC/PVA AND HEC/PVA/COLLAGEN NANOFIBERS SCAFFOLDS	62
4.1.1	Introduction	62
4.1.2	Morphology of HEC/PVA nanofibrous scaffolds	62
4.1.3	ATR-FTIR study	66
4.1.4	TGA measurements	68
4.1.5	DSC study	72
4.1.6	Mechanical properties	75
4.2	<i>IN VITRO</i> DEGRADATION STUDY OF HEC/PVA AND HEC/PVA/COLLAGEN NANOFIBERS SCAFFOLDS	77
4.2.1	Introduction	77
4.2.2	Morphological changes of nanofibers scaffold.	77
4.2.3	Weight loss, swelling ratio and pH value analysis	80
4.2.4	ATR-FTIR spectra analysis	84
4.2.5	DSC study	86
4.2.6	Mechanical characterization	88
4.3	MICROSTRUCTURE STUDY OF HEC/PVA POROUS SCAFFOLDS	90
4.3.1	Introduction	90
4.3.2	Microstructure of scaffolds	90
4.3.3	Porosity of scaffolds	92
4.3.4	Swelling ratio studies	93
4.3.5	<i>In vitro</i> degradation studies	94
4.3.6	ATR-FTIR spectroscopy analysis	95
4.3.7	Thermogravimetric (TGA) studies	97
4.3.8	Differential scanning calorimetry (DSC) study	99
4.3.9	Mechanical properties	101
4.4	STUDY OF HEC/SILVER NANOPARTICLES POROUS SCAFFOLDS	103
4.4.1	Introduction	103
4.4.2	Microstructure of HEC/AgNPs scaffolds	103
4.4.3	Porosity studies	105
4.4.4	Swelling ratio studies	106
4.4.5	<i>In vitro</i> degradation studies	107
4.4.6	UV-Vis absorbance spectroscopy	108
4.4.7	ATR-FTIR studies	109
4.4.8	TGA and DrTGA analysis	111
4.4.9	DSC study	113
4.5	Conclusion	114

CHAPTER 5	CELL CULTURE STUDIES ON NANOFIBERS AND FREEZE-DRIED SCAFFOLDS FOR SKIN TISSUE ENGINEERING APPLICATIONS	115
5.1	Introduction	115
5.2	Cells morphology studies	115
5.2.1	A375 cytotoxicity studies of HEC/PVA nanofibrous scaffolds	115
5.2.2	hFB cytotoxicity studies of HEC/PVA HEC/PVA/collagen electrospun nanofibrous scaffolds	117
5.2.3	hFB cells morphology on HEC/PVA porous scaffolds	118
5.2.4	hFB cells morphology on HEC/silver nanoparticles scaffolds	121
5.3	Cells proliferation studies	123
5.3.1	A375 cells proliferation studies on HEC/PVA nanofibrous scaffolds	123
5.3.2	hFB cells proliferation studies on HEC/PVA and collagen nanofibrous scaffolds	125
5.3.3	hFB cells proliferation studies on HEC/PVA porous scaffolds	126
5.3.4	hFB cells proliferation studies on HEC/silver nanoparticles scaffolds	128
5.4	Conclusion	129
CHAPTER 6	SUMMARY AND RECOMMENDATIONS	130
6.1	Summary	130
6.2	Recommendations for future studies	132
	REFERENCES	134
	ACHIEVEMENTS	160

LIST OF TABLES

Table No.	Title	Page
2.1	Examples of some commercially available skin substitutes	13
3.1	Summarized of samples prepared and incubation time points for cell culture studies in this work	59
4.1	Electrospinning parameters for HEC/PVA nanofibers and their corresponding average fiber diameter	64
4.2	TGA and DrTGA for polymer blends (CL-crosslinked, NCL- non-crosslinked)	72
4.3	DSC data and the characteristics (CL-crosslinked, NCL- non-crosslinked)	74
4.4	Mechanical data observed for the electrospun nanofibers (CL-crosslinked, NCL-non-crosslinked)	76
4.5	DSC data and the characteristics observed for the electrospun HEC/PVA and HEC/PVA/collagen nanofibers before and after <i>in vitro</i> degradation	86
4.6	Mechanical data of HEC/PVA and HEC/PVA/collagen nanofibers before and after degradation for up to 12 weeks	90
4.7	TGA and DrTGA data for HEC and PVA scaffolds	97
4.8	DSC data and the characteristics observed for the HEC, PVA and HEC/PVA blend samples	101
4.9	Mechanical data observed for the HEC, PVA and HEC/PVA blend samples	102
4.10	TGA and DrTGA data for HEC/AgNPs scaffolds	111
4.11	DSC data and the characteristics of HEC/PVA composites scaffold	114

LIST OF FIGURES

Figure No.	Title	Page
2.1	The structure of human skin	8
2.2	Evolution of biomaterials	19
2.3	Molecular structure of HEC	26
2.4	Molecular structure of PVA	27
2.5	Chemical structure of PVA and glutaraldehyde cross-linking	28
2.6	Triple-helical structure of collagen	29
3.1	Summary of research methodology implemented in this work	35
3.2	HEC/PVA (50:50) blended solution	37
3.3	HEC with 0.8% silver nanoparticles blended solution	38
3.4	Schematic diagram of the basic setup for electrospinning and Taylor cone Formation	40
3.5	Photograph of electrospinning machine, Electroris	40
3.6	Photograph of freeze-dryer machine, Labconco	42
3.7	The (a) HEC/PVA and (b) HEC/AgNPs freeze-dried scaffolds	43
3.8	Schematic diagram of a SEM	44
3.9	Photograph of SEM, Zeiss EVO 50	45
3.10	Graphical representation of multiple ATR reflection	46
3.11	Photograph of ATR-FTIR, Perkin-Elmer	47
3.12	Schematic diagram of TG-DTA system	47
3.13	Photograph of TGA	48
3.14	Schematic diagram of DSC	50

3.15	DSC thermograms	50
3.16	Photographs of DSC, TA instruments	50
3.17	Stress-strain curve diagram	52
3.18	Photograph of universal testing machine, Shimadzu	53
3.19	UV-Vis spectrophotometer, Thermoscientific	54
3.20	Collective oscillations of free electrons due to applied electric field	55
3.21	Summarize of cell culture study	57
3.22	Cell culture studies of HEC/PVA nanofibers scaffolds at different weight ratios	58
3.23	Photograph of ELISA microplate reader, VersaMax™	60
3.24	MTS assay of HEC/PVA nanofibers scaffolds at different weight ratios	61
4.1	Plot of the viscosity of the solution with respect to the wt% of the HEC/PVA (a) 50:50, (b) 40:60, (c) 30:70 in the solution	63
4.2	SEM images of HEC nanofibers mats (white arrow indicates the droplets)	64
4.3	SEM images and diameter distribution of electrospun HEC/PVA nanofibers: (a,b) H50P50, (c,d) H40P60, (e,f) H30P70, (g,h) with collagen	65
4.4	ATR-FTIR spectra of (i) non-crosslinked and (ii) crosslinked electrospun HEC/PVA nanofibers: (a) H50P50, (b) H40P60, (c) H30P70, (d) with collagen	67 - 68
4.5 (a*-d*)	TGA and drTGA curves for non-crosslinked electrospun HEC/PVA nanofibers: (a) H50P50, (b) H40P60, (c) H30P70, (d) with collagen	69
4.5 (a-d)	TGA and drTGA curves for crosslinked electrospun HEC/PVA nanofibers: (a)H50P50, (b) H40P60, (c) H30P70, (d) with collagen	71
4.6	DSC thermograms for (i) non-crosslinked and (ii) crosslinked electrospun HEC/PVA nanofibers:(a) H50P50, (b) H40P60, (c) H30P70, (d) with collagen	74

4.7	Stress-strain curves for (i) non-crosslinked and (ii) crosslinked electrospun HEC/PVA nanofibers: (a) H50P50, (b) H40P60, (c) H30P70, (d) with collagen	76
4.8	SEM micrographs of HEC/PVA and HEC/PVA/collagen nanofibrous scaffolds after degradation in DMEM media at different time	78
4.9	SEM micrographs of HEC/PVA and HEC/PVA/collagen nanofibrous scaffolds after <i>in vitro</i> degradation in PBS media at different time	79
4.10	Weight loss of HEC/PVA and HEC/PVA/collagen nanofibrous scaffolds after degradation in PBS and DMEM media for up to 12 weeks	81
4.11	Swelling ratio of HEC/PVA and HEC/PVA/collagen nanofibrous scaffolds after degradation in PBS and DMEM media for up to 12 weeks	82
4.12	pH value of HEC/PVA and HEC/PVA/collagen nanofibers scaffold after degradation for up to 12 weeks in (a) DMEM and (b) PBS solution	83
4.13	ATR-FTIR analysis before and after degradation for incubation up to 12 weeks. (a) HEC/PVA/collagen nanofibers immersed in DMEM solution; (b) HEC/PVA nanofibers immersed in DMEM solution; (c) HEC/PVA/collagen nanofibers immersed in PBS solution; (d) HEC/PVA nanofibers immersed in PBS solution	85
4.14	DSC thermogram before and after degradation for incubation up to 12 weeks: (a) HEC/PVA/collagen nanofibers immersed in DMEM solution; (b) HEC/PVA nanofibers immersed in DMEM solution; (c) HEC/PVA/collagen nanofibers immersed PBS solution; (d) HEC/PVA nanofibers immersed PBS solution	87
4.15	Stress-strain curves (i) before and (ii) after degradation for incubation up to 12 weeks: (a) HEC/PVA/collagen nanofibers immersed in DMEM solution; (b) HEC/PVA nanofibers immersed in DMEM solution; (c) HEC/PVA/collagen nanofibers immersed PBS solution; (d) HEC/PVA nanofibers immersed PBS solution.	89
4.16	SEM micrographs of interconnected porous scaffolds (a) pure HEC, (b) HEC/PVA (2:1), (c) HEC/PVA (1:1), (d) HEC/PVA (1:2) and (e) pure PVA	91

4.17	Porosity of different porous scaffolds	93
4.18	Swelling ratio of pure HEC, HEC/PVA (2:1), HEC/PVA (1:1), HEC/PVA (1:2) and pure PVA porous scaffolds	94
4.19	Percentage of weight loss of pure HEC, HEC/PVA (2:1), HEC/PVA (1:1), HEC/PVA (1:2) and pure PVA porous scaffolds	95
4.20	ATR-FTIR analysis for (a) pure HEC, (b) HEC/PVA (2:1), (c) HEC/PVA (1:1), (d) HEC/PVA (1:2) and (e) pure PVA porous scaffolds	96
4.21	TGA and DrTGA analysis for (a) pure HEC, (b) HEC/PVA (2:1), (c) HEC/PVA (1:1), (d) HEC/PVA (1:2) and (e) pure PVA porous scaffolds	99
4.22	DSC analysis for (a) HEC only, (b) HEC/PVA (2:1), (c) HEC/PVA (1:1), (d) HEC/PVA (1:2) and (e) PVA scaffolds	100
4.23	Stress-strain curves for (a) HEC only, (b) HEC/PVA (2:1), (c) HEC/PVA (1:1), (d) HEC/PVA (1:2) and (e) PVA scaffolds	102
4.24	(i) Photograph of HEC/AgNPs solution obtained at different concentrations of AgNO ₃ , (ii) macroscopic appearance of HEC/AgNPs scaffold, SEM micrograph of HEC/AgNPs scaffold at different concentrations of Ag (a) 0.4%, (b) 0.8%, (c) 1.6 %.	104 - 105
4.25	Porosity of HEC/AgNPs scaffolds with different Ag concentrations at 0.4%, 0.8% and 1.6%	106
4.26	Swelling ratio of HEC/AgNPs scaffolds with different Ag concentrations at 0.4%, 0.8% and 1.6%	107
4.27	Weight loss of degrading HEC/AgNPs scaffolds with different Ag concentrations at 0.4%, 0.8% and 1.6%	108
4.28	UV-Vis absorption spectra of HEC/AgNPs scaffolds	108
4.29	ATR-FTIR studies for HEC with different concentrations of Ag (a) 0.4%, (b) 0.8% and (c) 1.6% porous scaffolds	110
4.30	TGA and DrTGA analysis for HEC with different concentrations of Ag (a) 0.4%, (b) 0.8% and (c) 1.6% porous scaffolds	112
4.31	DSC study for HEC with different concentrations of Ag (a)	114

	0.4%, (b) 0.8% and (c) 1.6% porous scaffolds	
5.1	SEM micrographs of human A375 melanoma cells attached on nanofibrous scaffolds: (a) H50P50, (b) H40P60, (c) H30P70	116
5.2	SEM micrographs of hFB cells attached on HEC/PVA and HEC/PVA/collagen after 2, 4 and 7 days incubation	118
5.3 (i)	SEM micrograph images of hFB cells attached on (a) pure HEC, (b) HEC/PVA (2:1), (c) HEC/PVA (1:1), (d) HEC/PVA (1:2) and (e) pure PVA scaffolds after day 1 cell culture (black arrow indicates the growth cells)	119
5.3 (ii)	SEM micrograph images of hFB cells attached on (a) pure HEC, (b) HEC/PVA (2:1), (c) HEC/PVA (1:1), (d) HEC/PVA (1:2) and (e) pure PVA scaffolds after day 4 cell culture (black arrow indicates the growth cells)	120
5.3 (iii)	SEM micrograph images of hFB cells attached on (a) pure HEC, (b) HEC/PVA (2:1), (c) HEC/PVA (1:1), (d) HEC/PVA (1:2) and (e) pure PVA scaffolds after day 7 cell culture (black arrow indicates the growth cells)	121
5.4	SEM micrograph images of hFB cells attached on HEC with different concentrations of Ag (a) 0.4%, (b) 0.8% and (c) 1.6% scaffolds after 4 h and 24 h incubation period (black arrow indicates the growth cells)	122
5.5	Graph showing human A375 melanoma viability after 1, 3 and 7 days of incubation (1×10^5 cells/well in complete DMEM) at different weight ratios of nanofibrous scaffolds. (<i>H</i> -HEC content, <i>P</i> -PVA content)	124
5.6	Graph showing human fibroblast viability after 2, 4 and 7 days of incubation (1×10^5 cells/well in complete MEM) at different weight ratios of nanofibrous scaffolds	126
5.7	Graph showing human fibroblast viability after 2, 4 and 7 days of incubation (1×10^5 cells/well in complete MEM) at different weight ratios of HEC/PVA scaffolds	127
5.8	Graph showing human fibroblast viability after 4, 12 and 24 h of incubation (1×10^6 cells/well in complete MEM) of HEC in different concentrations of Ag (a) 0.4%, (b) 0.8% and (c) 1.6% scaffolds	128

LIST OF SYMBOLS

χ_c	Crystallinity
σ	Stress
ε	Strain
E	Young's modulus
ΔH	Enthalpy of fusion
F	Force
A_o	Cross-sectional area
L_f	Final length
L_o	Original length
ΔH_f	Enthalpy of fusion
ΔH_f^o	Enthalpy of fusion of 100% crystallization
ΔH_m	Heat of fusion
W_o	Initial weight
W_t	Wet weight
W_d	Dry weight
V_1	Known volume
V_2	Total of new volume after sample immersion
V_3	Total of new volume after sample removal
T	Temperature
T_g	Glass transition temperature
T_m	Melting temperature
d	Diameter
λ	Wavelength

LIST OF ABBREVIATIONS

AgNO ₃	Silver nitrate
AgNP	Silver nanoparticle
Al ₂ O ₃	Alumina
ATR-FTIR	Attenuated total reflectance Fourier transform infrared spectroscopy
Ca ₃ (PO ₄) ₂	Beta-tricalcium phosphate
CL	Cross-linking
Co	Cobalt
Cr	Chromium
DHT	Dehydrothermal treatment
DMEM	Dulbecco's modified eagle medium
DNA	Deoxyribonucleic acid
DSC	Differential scanning calorimetry
ECM	Extracellular matrix
EDC	1-ethyl-3-(3-dimethylamino propyl) carbodiimide hydrochloride
FBS	Fetal bovine Serum
FDA	Food and Drug Administration
GA	Glutaraldehyde
GAG	Glycosaminoglycan
HA	Hydroxyapatite
HEC	Hydroxyethyl cellulose
hFB	Human fetal fibroblast
HUVECs	Human umbilical vein endothelial cells
MEM	Minimum essential media
NaBH ₄	Sodium borohydride
NCL	Non-cross-linking
PBS	Phosphate buffered saline
PCL	Polycaprolactone
PE	Poly(ethylene)

PET	Poly(ethylene terephthalate)
PFF	Polypropylene fumarate
PGA	Polyglycolic acid
PLA	Poly(lactic) acid
PLGA	Poly(lactic-co-glycolic acid)
PLLA	Poly-L-lactide acid
PMMA	Poly(methyl methacrylate)
PTFE	Poly(tetrafluoroethylene)
PVA	Poly(vinyl) alcohol
RNA	Ribonucleic acid
SEM	Scanning electron microscope
SPR	Surface Plasmon resonance
TCP	Tricalcium phosphate
TGA	Thermogravimetric analysis
Ti	Titanium
UTM	Universal testing machine
UV	Ultraviolet
ZrO ₂	Zirconia

CHAPTER 1

INTRODUCTION

1.1 BACKGROUND

Skin is the largest organ of the human body. It serves as a barrier against pathogenic microbial agents, UV irradiation, mechanical disturbances, and protects substantial loss of body fluids. Loss of skin integrity arising from acute trauma, chronic wounds and severe burns may result in organ malfunction or even death (Sangur, 2010). Tissue engineering can be defined as a combination of multidisciplinary fields that applies the principles and systematic procedures of engineering and biological sciences that restore, maintain or improve the structure and functions of damaged tissue (Sachlos and Czernuszka, 2003). The emergence of tissue engineered skin replacements have conquered several limitations over conventional tissue transplants of autograft, allograft and xenograft such as preventing additional surgical procedures, eliminating the chance of graft rejection or the transmission of infection diseases (Böttcher-Haberzeth et al., 2010). For these reasons, the use of artificial skin equivalents becomes great and extensively grown in skin tissue markets. Moreover, since skin transplant becomes clinically practicable, the demand for safe, affordable and stable product always exceeds the available supply. In 2009, Medtech Insight reported that the potential US market for tissue engineered skin replacement and substitutions total approximately \$18.9 billion based on target population of approximately 5.0 million people (Medtech Insight, 2014). This target population is expecting to reach 6.4 million people that result in approximately \$24.3 billion by 2019. In skin tissue market, a wide variety of skin substitutes such as Alloderm®, Graftjacket® and Gammagraft® have been clinically tested and approved by Food and Drug Administration (FDA). These commercial products are introduced into the market especially for superficial, partial and deep burn

wounds and chronic ulcers. However, most of these bioengineered skin substitutes necessitate high cost, expertise and experience that might confer difficulty and financial issue to some patients. For instance, the cost of Apligraf® is about \$ 1,000 to \$ 1, 200 per use and at least \$2000 is needed for an 8'' x 10'' sheet of Integra™ skin. In other cases, the price of Epicel™ including operation procedure can range from \$ 6,000 to \$10,000 per 1% total body area surface.

The basic concepts of tissue engineering are to harvest a small biopsy of the specific cells from the donor site and expand the cells in a Petri dish. After confluence, the cells are seeded on a polymeric scaffold for *in vitro* cell culture study and consequently transplanted into the defect area of a patient's body (Arya et al., 2009). Three main factors that contribute to the success of tissue engineering are cells, scaffolds and cell-scaffold interactions that play a major role in organizing and assembling subsequent function into particular tissues. Nowadays, research using nano biomaterials as scaffolds in skin tissue engineering is tremendously increasing as these biomaterials mimic the structure of extracellular matrices and provide a platform for cell attachment, differentiation and proliferation. Biopolymer used to construct three-dimensional scaffolds should be biocompatible, biodegradable, highly porous in structure, and possessing adequate mechanical strength and stability. The nanoscale biomaterials are produced *via* several methods including self-assembly, template assisted synthesis, drawing, phase separation and electrospinning (Kumbar et al., 2008). However, electrospinning gains most interest among researchers because of the capability to fabricate a variety of polymeric nanofibers (Huang et al., 2003). Electrospinning is a technique that produces fibers in nanometer length and interconnected pores that closely resemble the topography features of ECM. It is a versatile technique to produce nano and microfibers from polymer solutions or melts in the range of 30-200 nm through the action of high electric fields (Taylor et al., 2006; Reneker and Chun, 1996 and Yarin et al., 2001). The morphology and properties of the nanofibers can be varied by changing the process parameters such as solution viscosity and conductivity, applied voltage, average molecular weight of the polymer and the distance between the needle and the collector plate (Zong et al., 2002 and Shin et al., 2001). The main attractions of the electrospun nanofibers are their unique properties such as high surface area-to-volume ratio, high porosity, and their diameter, which is in

the nanometer range. Scaffold fabrication by lyophilization or freeze-drying is another convenient technique to produce highly interconnected micropore structures. Freeze-drying removes most of the water from the sample under vacuum to obtain highly porous architecture scaffolds. Porous microstructures are very important especially for nutritional support and removal of metabolic waste produced by the populated cells in the injured site (Xiao et al., 2011). The microstructure of the design scaffolds have to mimic the native structure of the extracellular matrix (ECM) to support and enhance the growth of new tissue during the recovery period.

Although current skin engineered constructs seem to increase healing rates of burn or chronic injuries, the dire demands on less complex tissue-engineered construct that are relatively cost-effective with minimal risk of infection still remain as great challenges. Until this day, no ideal skin substitute is successfully achieved, thus consequently leading to continuous studies in finding the optimal criteria for suitable skin substitute equivalent. In regard to this, it is vital to understand the influence of polymer scaffolds on cellular function and behaviour. Therefore, further research should be executed to compare and characterize different types of skin substitutes and evaluate the substrates' biological response for skin tissue engineering applications.

1.2 PROBLEM STATEMENT

Skin tissue engineering using scaffolds overcomes the limitations from several wound healing processes like autografts, allografts and xenografts (Groeber et al., 2011 and Macneil, 2008). The advent of skin tissue substitutes revolutionized the therapeutic potential for critical wounds and wounds that are not amenable to primary closure. Although conventional transplant revealed efficient performance, they still present several limitations such as double surgery site, immune rejection, risk of infection and viral transmission. At worst, most organ recipients need to take drugs for suppression of natural immune responses, which may lead to immunological imbalances or even tumor growth in the long term (Zhang and Michniack-Khon, 2012).

In previous research, scaffolds that have suitable surface chemistry and excellent mechanical strength have been fabricated from several natural and synthetic polymers,

which includes chitin, chitosan, polyurethane (PU), nylon, polyglycolic acid/polylactic acid (PGA/PLA), poly(L-lactide) (PLLA), polycaprolactone (PCL), and copolymer poly(ethyleneglycolterephthalate)-poly(butylenes terephthalate) (Dai et al., 2004 and Beumer et al., 1993). Fabrication of nanomaterials from most of these polymers require harmful or organic acid solvents like acrylic acid, acetic acid, chloroform, trifluoroacetic acid and 1,1,1,3,3,3-hexafluoro-2-propanol, give difficulties to researchers to handle the toxic solvents (Zhang et al., 2006, Liu et al., 2011 and Huang et al., 2003). In addition, although there are a number of commercially bioengineered skin substitutes available in the market- as will be outlined in Chapter 2 of this thesis- due to high prices, poor vascularization and toxicity issues during synthesis process, there are tremendous demands for tissue engineered biopolymer scaffolds, which are comparably cost-effective, better cell-tissue interaction and constructed in an environmentally friendly way. As a key to address these issues, designation and fabrication of scaffolds that possess as accurate as possible the characteristics of native ECM with no adverse effects on the damaged skin are immensely favourable.

1.3 SIGNIFICANCE OF STUDIES

In this work, HEC nanomaterials were prepared using a 'green' chemistry approach in a straightforward procedure. The HEC solutions were prepared using water as the only solvent. The HEC scaffolds were synthesized using two simple techniques, which are electrospinning and freeze-drying. This research aims to develop non-toxic, biocompatible, and biodegradable scaffolds that can potentially be commercialized as skin substitute equivalents. Since a small amount of HEC powder can be processed to produce scaffolds in large scale, this novel material will be of high demand in tissue engineering markets that lack superior healing rate scaffolds with affordable prices. The findings of this work will merit the medical community especially those who work in skin tissue engineering as well as low and middle-class patients who bear acute burn injuries, ulcers, and venous stasis that prerequisite cost-effective scaffolds with rapid healing response.

1.4 RESEARCH OBJECTIVES

The main objectives of this thesis are:

- i. To fabricate scaffolds based on HEC/PVA, HEC/PVA/collagen and HEC/Ag nanoparticles using an aqueous polymeric-solution-based electrospinning and freeze-drying techniques.
- ii. To evaluate the physical, chemical, thermal and mechanical properties of all scaffolds produced.
- iii. To investigate the potential of the produced scaffolds as substrates for skin tissue engineering applications.

1.5 RESEARCH SCOPE

The following research scopes are essential to achieve the first objective:

- i. To optimize the viscosity of the electrospun polymer solution for developing uniform, beadless and continuous nanofibers.
- ii. To optimize the electrospinning parameters such as high applied-voltage, feed rate, tips-to-collector distance and rotation speed that tailor the diameter of nanofibers.
- iii. To find the effect of different weight ratios of HEC/PVA scaffolds that offer the best performance as skin tissue engineered scaffolds.
- iv. To optimize the concentration of HEC as a reducing agent in the formation of silver nanoparticles and also the concentration of AgNO_3 that would generate an ideal HEC/silver nanoparticle based scaffold.

The following research scopes are necessary to achieve the second objective:

- i. To identify surface morphology *via* SEM images and to measure the diameter of the fiber and the pore size of all scaffolds using ImageJ software.
- ii. To recognize the functional groups of all scaffolds using ATR-FTIR spectra.
- iii. To examine the thermal stability and decomposition behaviour of scaffolds using TGA and DSC.

- iv. To study the strength of scaffolds by analyzing the stress-strain curves using UTM.
- v. To identify the pore size and porosity of the freeze-dried scaffolds.
- vi. To investigate the degradation behaviour of electrospun polymer scaffolds in PBS and DMEM at different time points. The analysis will involve pH changes of the solutions, weight loss and swelling ratio.

Finally, the following research scopes are necessary to achieve the third objective:

- i. To investigate the cellular biocompatibility by carrying out *in vitro* cell culture studies and measure the absorbance value using MTT and MTS assays.
- ii. To determine the adherence, differentiation and proliferation of skin melanoma and fibroblast cells on the scaffolds and observe surface morphological changes by SEM.
- iii. To configure the potential incorporation of collagen with HEC/PVA electrospun mats that might display positive response towards skin cells.
- iv. To compare the effect of different weight ratios of HEC/PVA and HEC with different concentrations of AgNO_3 as potential substrates for skin tissue engineering applications.

1.6 THESIS OUTLINE

The following is a brief aspect of the contents in this thesis. Chapter 2 provides a comprehensive overview of former and recent research on skin tissue engineering and details of polymeric materials involved in the research. Chapter 3 presents the experimental method used in this work and the working principle of the instruments used for characterization. Chapter 4 discusses the synthesis and characterization of HEC/PVA, HEC/PVA/collagen and HEC/AgNPs scaffolds. Chapter 5 outlines the cell culture studies on the scaffolds for skin tissue engineering application. Finally, the summary of this work and the recommendations for future work are given in Chapter 6.

CHAPTER 1

INTRODUCTION

1.1 BACKGROUND

Skin is the largest organ of the human body. It serves as a barrier against pathogenic microbial agents, UV irradiation, mechanical disturbances, and protects substantial loss of body fluids. Loss of skin integrity arising from acute trauma, chronic wounds and severe burns may result in organ malfunction or even death (Sangur, 2010). Tissue engineering can be defined as a combination of multidisciplinary fields that applies the principles and systematic procedures of engineering and biological sciences that restore, maintain or improve the structure and functions of damaged tissue (Sachlos and Czernuszka, 2003). The emergence of tissue engineered skin replacements have conquered several limitations over conventional tissue transplants of autograft, allograft and xenograft such as preventing additional surgical procedures, eliminating the chance of graft rejection or the transmission of infection diseases (Böttcher-Haberzeth et al., 2010). For these reasons, the use of artificial skin equivalents becomes great and extensively grown in skin tissue markets. Moreover, since skin transplant becomes clinically practicable, the demand for safe, affordable and stable product always exceeds the available supply. In 2009, Medtech Insight reported that the potential US market for tissue engineered skin replacement and substitutions total approximately \$18.9 billion based on target population of approximately 5.0 million people (Medtech Insight, 2014). This target population is expecting to reach 6.4 million people that result in approximately \$24.3 billion by 2019. In skin tissue market, a wide variety of skin substitutes such as Alloderm®, Graftjacket® and Gammagraft® have been clinically tested and approved by Food and Drug Administration (FDA). These commercial products are introduced into the market especially for superficial, partial and deep burn

wounds and chronic ulcers. However, most of these bioengineered skin substitutes necessitate high cost, expertise and experience that might confer difficulty and financial issue to some patients. For instance, the cost of Apligraf® is about \$ 1,000 to \$ 1, 200 per use and at least \$2000 is needed for an 8'' x 10'' sheet of Integra™ skin. In other cases, the price of Epicel™ including operation procedure can range from \$ 6,000 to \$10,000 per 1% total body area surface.

The basic concepts of tissue engineering are to harvest a small biopsy of the specific cells from the donor site and expand the cells in a Petri dish. After confluence, the cells are seeded on a polymeric scaffold for *in vitro* cell culture study and consequently transplanted into the defect area of a patient's body (Arya et al., 2009). Three main factors that contribute to the success of tissue engineering are cells, scaffolds and cell-scaffold interactions that play a major role in organizing and assembling subsequent function into particular tissues. Nowadays, research using nano biomaterials as scaffolds in skin tissue engineering is tremendously increasing as these biomaterials mimic the structure of extracellular matrices and provide a platform for cell attachment, differentiation and proliferation. Biopolymer used to construct three-dimensional scaffolds should be biocompatible, biodegradable, highly porous in structure, and possessing adequate mechanical strength and stability. The nanoscale biomaterials are produced *via* several methods including self-assembly, template assisted synthesis, drawing, phase separation and electrospinning (Kumbar et al., 2008). However, electrospinning gains most interest among researchers because of the capability to fabricate a variety of polymeric nanofibers (Huang et al., 2003). Electrospinning is a technique that produces fibers in nanometer length and interconnected pores that closely resemble the topography features of ECM. It is a versatile technique to produce nano and microfibers from polymer solutions or melts in the range of 30-200 nm through the action of high electric fields (Taylor et al., 2006; Reneker and Chun, 1996 and Yarin et al., 2001). The morphology and properties of the nanofibers can be varied by changing the process parameters such as solution viscosity and conductivity, applied voltage, average molecular weight of the polymer and the distance between the needle and the collector plate (Zong et al., 2002 and Shin et al., 2001). The main attractions of the electrospun nanofibers are their unique properties such as high surface area-to-volume ratio, high porosity, and their diameter, which is in

the nanometer range. Scaffold fabrication by lyophilization or freeze-drying is another convenient technique to produce highly interconnected micropore structures. Freeze-drying removes most of the water from the sample under vacuum to obtain highly porous architecture scaffolds. Porous microstructures are very important especially for nutritional support and removal of metabolic waste produced by the populated cells in the injured site (Xiao et al., 2011). The microstructure of the design scaffolds have to mimic the native structure of the extracellular matrix (ECM) to support and enhance the growth of new tissue during the recovery period.

Although current skin engineered constructs seem to increase healing rates of burn or chronic injuries, the dire demands on less complex tissue-engineered construct that are relatively cost-effective with minimal risk of infection still remain as great challenges. Until this day, no ideal skin substitute is successfully achieved, thus consequently leading to continuous studies in finding the optimal criteria for suitable skin substitute equivalent. In regard to this, it is vital to understand the influence of polymer scaffolds on cellular function and behaviour. Therefore, further research should be executed to compare and characterize different types of skin substitutes and evaluate the substrates' biological response for skin tissue engineering applications.

1.2 PROBLEM STATEMENT

Skin tissue engineering using scaffolds overcomes the limitations from several wound healing processes like autografts, allografts and xenografts (Groeber et al., 2011 and Macneil, 2008). The advent of skin tissue substitutes revolutionized the therapeutic potential for critical wounds and wounds that are not amenable to primary closure. Although conventional transplant revealed efficient performance, they still present several limitations such as double surgery site, immune rejection, risk of infection and viral transmission. At worst, most organ recipients need to take drugs for suppression of natural immune responses, which may lead to immunological imbalances or even tumor growth in the long term (Zhang and Michniack-Khon, 2012).

In previous research, scaffolds that have suitable surface chemistry and excellent mechanical strength have been fabricated from several natural and synthetic polymers,

CHAPTER 3

MATERIALS AND METHODS

This chapter discusses in detail the research methodology, which comprise of various methods and materials being employed in the present research. The steps include the synthesis and fabrication of nanofibers and porous freeze-dried scaffolds, the tools and techniques used for the characterization of the material, the procedures involved in the cell-culture experiment, and the techniques used to measure cell proliferation on the scaffolds.

3.1 RESEARCH METHODOLOGY

Flowchart 3.1 pointed out the research methodology being practiced in this work. The materials were synthesized by electrospinning and freeze-drying techniques using aqueous polymeric solution; the parameters for both techniques were optimized to obtain fibers in nanoscale and highly porous freeze-dried scaffolds. The scaffolds were further characterized based on their physical, chemical, thermal and mechanical properties. All scaffolds underwent cell culture studies to check their cell responses and compatibility along incubation periods. The techniques used for synthesis, fabrication, characterization, and testing are further discussed in this chapter.

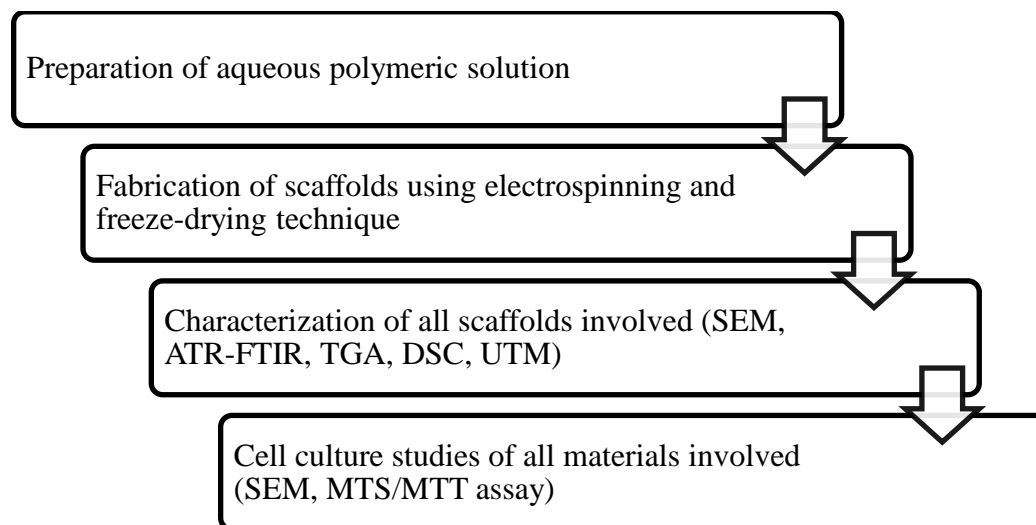


Figure 3.1: Summary of research methodology implemented in this work

3.2 MATERIALS PREPARATION

All materials used in this work are commercially available. Hydroxyethyl cellulose (CAS number: 9004-62-0) was purchased from Merck-Schucardt, Germany. Hydroxyethyl cellulose ($M_w = 250,000$) and silver nitrate (AgNO_3) were purchased from Sigma-Aldrich, USA. Poly (vinyl) alcohol ($M_w = 95,000$) was purchased from ACROS, New Jersey, USA. Collagen type I, liquid rat tendon excised from tail (0.02N acetic acid, pH 3.67) was purchased from Merck-Millipore Corporation, Billerica, MA, USA. Analytical reagent grade glutaraldehyde (GA) solution (25% aqueous solution) was purchased from Merck-Schucardt, Germany. Phosphoric acid was purchased from Merck.KGaA-Darmstadt, Germany. Acetone was purchased from R&M Marketing, Essex, UK. Phosphate buffer saline (PBS) was purchased from Gibco Life Technologies, USA. Dulbecco's Modified Eagle Medium (DMEM) was purchased from Life Technologies, USA. All the chemicals were of highest purity and used without further purification. All the solutions were prepared using Millipore water.

3.3 PREPARATION OF ELECTROSPINNING AQUEOUS POLYMERIC SOLUTIONS

Biomaterial scaffolds with a large amount of water diffused in three dimensional polymeric networks are highly needed in biomedical and health applications (Deligkaris et al., 2010). Many water soluble synthetic polymers such as poly (vinyl) alcohol (PVA) (Zhou et al., 2010), poly (vinyl pyrrolidone) (PVP) (Elashmawi and Abdel Baieth, 2012 and Shi et al., 2014) and poly ethylene glycol (PEG) (El-Ghalbzouri et al., 2004) are combined with natural polymers to improve cell-recognition moieties, mechanical properties and high processability (Arya et al., 2009). Combination of natural polymer with synthetic polymers like PVA, a biodegradable, non-toxic and non-carcinogenic hydrogel, improves the spinnability and mechanical properties such as elasticity and elongation (Mansur and Mansur, 2007). In addition, blending of synthetic and natural biopolymers from three or more components reveal tremendous results in cell-scaffold behaviour (Sionkowska, 2011). In this research, HEC was blended with PVA and collagen to improve their spinnability as well as the cell response towards skin cells.

3.3.1 Synthesis of HEC/PVA and HEC/PVA/collagen nanofibers scaffolds

The HEC solution with a concentration of 5 wt% was prepared by dissolving 5 g of HEC powder in 100 ml of Millipore water for 2 h at room temperature until a clear solution was obtained with a slight increase in viscosity. PVA solution of 15 wt% was prepared by dissolving 15 g of PVA granules in 100 ml of Millipore water and stirring at 80 °C for 2 h. Both solutions were stirred continuously for 12 h at room temperature to ensure complete mixing and eventually obtain a homogeneous solution. HEC was then blended in PVA solution with 3 different weight ratios of HEC/PVA, which are 50:50, 40:60 and 30:70 and stirred overnight to get a homogeneous mixture for electrospinning. The HEC/PVA (50:50) blended aqueous polymeric solution is shown in Figure 3.2. For ternary blend system, collagen solution with concentration of 0.38 % was added into the HEC/PVA solution in the ratio of 1:1:1 and stirred continuously to get homogenous blend solution.